Inorganic Chemistry
Cite This: Inorg. Chem. XXXX, XXX, XXX–XXX
Article
pubs.acs.org/IC

Diverse Functionalization of Ruthenium-Chelated 2-Picolylamines: Oxygenation, Dehydrogenation, Cyclization, and *N*-Dealkylation

Sanjib Panda,* Arijit Singha Hazari, Manish Gogia, and Goutam Kumar Lahiri*

Department of Chemistry, Indian Institute of Technology (IIT) Bombay, Powai, Mumbai 400076, India

Supporting Information

ABSTRACT: "Chemical noninnocence" of metal-coordinated 2-picolylamine (PA) derivatives has been introduced upon its reaction with the metal precursor $[Ru^{II}(Cl)(H)(CO)(PPh_3)_3]$ under basic conditions. This in effect leads to the facile formation of metalated amide, imine, ring-cyclized pyrrole, and an N-dealkylated congener based on the fine-tuning of an amine nitrogen (N_{amine}) and a methylene center (C_α) at the PA backbone. It develops oxygenated L1′ in **1** and cyclized L4′ in **4** upon switching of the N_{amine} substituent of PA from aryl to an electrophilic pent-3-en-2-one moiety. On the other hand, imposing the substituent at the C_α position of PA modifies its reactivity profile, leading to a dehydrogenation (**2**/**3**) or *N*-dealkylation (**6**) process. The divergent reactivity profile of metalated PA is considered to proceed through a common dianionic intermediate. Further, a competitive scenario of C−H bond functionalization of coordinated PA versus the ligand-exchange process has been exemplified in the presence of external electrophile such as benzyl bromide or methylene iodide. Authentication of the product formation as well as elucidation of the reaction pathway has been addressed by their crystal structures and spectroscopic features in conjunction with the transition-state (TS) theory.

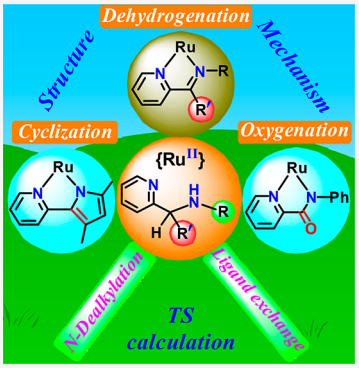

INTRODUCTION

Nitrogenous heterocycles, the skeletal moieties in numerous biologically active species and natural products, have received continuing research interest from the broader perspectives of its utility in synthetic chemistry.[1] Variegated strategies are therefore employed in procuring such diversified products. Among them, functionalization via the assistance of a metal ion is considered to be one of the facile synthetic protocols to introduce structural miscellany onto these substrate backbones.[2] In this regard, diversification of 2-picolylamine (PA)-derived molecular frameworks has gained profound attention because these are the important scaffolds of many natural products, synthetic drugs, and building blocks.[3] Besides, they have found widespread application in coordination chemistry because of their enriched donor ability and robust nature.[4] However, a few reports relating to the "non-spectator" feature (oxygenation and oxidative dehydrogenation) of the coordinated picolyl fragment in PA and its allied backbones are accounted for under special circumstances,[5] but the activation of PA toward cyclization still remains elusive.

In this context, the present paper demonstrates poorly explored multifarious reactivity strategies of ruthenium-coordinated PA and its structural analogues under basic conditions. It includes systematic alteration of the reactivity at the methylene center (C_α) of PA as a function of metal chelation as well as modulation of the substrate backbone (Scheme 1). This, in turn, leads to (i) aerial oxygenation ($CH_2 \rightarrow C{=}O$) of *N*-aryl-substituted PA to amide, (ii) formation of imine ($-CH-NH \rightarrow -C{=}N$) upon selective substitution at C_α of PA, and (iii) ring-closing scenario by integrating an electrophilic counterpart in its backbone, which, however, results in *N*-dealkylation upon affixing alkyl/aryl substitution at C_α. On the other hand, PA fails to react with the external electrophiles (E^+) and instead undergoes a ligand-exchange process. Structural and mechanistic details along with correlation of the reactivity have been authenticated by spectroscopic and theoretical details.

Scheme 1. Ruthenium-Chelation-Assisted Varying Functionalization of PA[a]

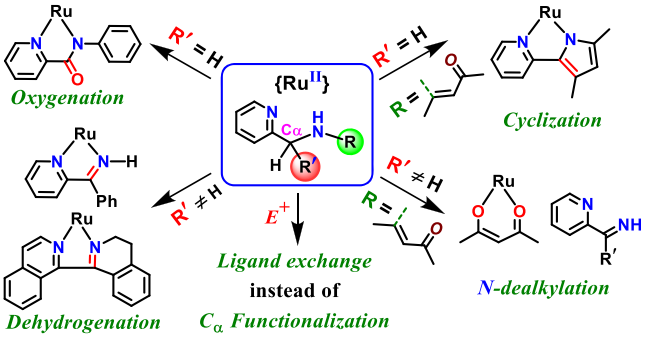

[a] E^+ stands for an external electrophile.

RESULTS AND DISCUSSION

Synthetic, Structural, and Spectroscopic Aspects. Complexes with the general formula $[Ru^{II}(H/Cl)(L')(CO)$-

Received: October 19, 2019

DOI: 10.1021/acs.inorgchem.9b03065
Inorg. Chem. XXXX, XXX, XXX–XXX

$(PPh_3)_2](ClO_4)_n$ (n = 0 for **1** and **4** and n = 1 for **2** and **3**) involving functionalized ligand moieties (L′ in Scheme 2) are

Scheme 2. Synthetic Outline for 1−6[a]

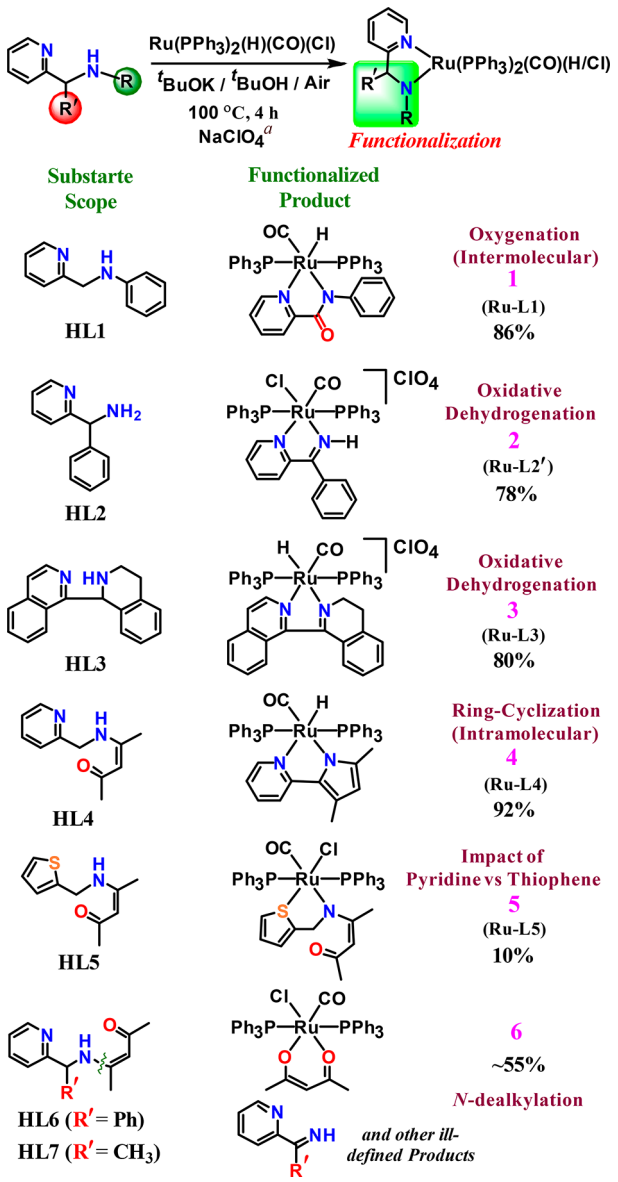

[a]$NaClO_4$ is required only for the synthesis of **2** and **3**.

obtained from the reactions of a 1:1 mixture of $[Ru^{II}(Cl)(H)(CO)(PPh_3)_3]$ and the respective PA-derived ligand precursors (HL) in refluxing *tert*-butyl alcohol (^{t}BuOH) in the presence of ^{t}BuOK base under aerobic conditions. The use of *N*-(pyridin-2-ylmethyl)aniline (**HL1** in Scheme 2) results in coordinated phenyl(picolinoyl)amide (**L1′**) in $[Ru^{II}(H)(L1')(CO)(PPh_3)_2]$ (**1**) via aerobic oxygenation at C_α in an intermolecular fashion. Involvement of aerial oxygen in the conversion sequence has been confirmed by an $^{18}O_2$-isotope-labeling experiment (Figure S2). In contrast, the reaction of $[Ru^{II}(Cl)(H)(CO)(PPh_3)_3]$ with C_α-substituted PA in phenyl(pyridin-2-yl)methanamine (**HL2**) and tetrahydro-1,1′-bis(isoquinoline) (**HL3**, a mimicked PA) leads to the corresponding imine counterparts **L2′** and **L3′** in isolated $[Ru^{II}(Cl)(L2')(CO)(PPh_3)_2]ClO_4$ (**2**) and $[Ru^{II}(H)(L3')(CO)(PPh_3)_2]ClO_4$ (**3**), respectively, where excess $NaClO_4$ is used to balance the charge of the complexes. However, the same reaction in the absence of a base under a N_2 atmosphere fails to extend the desired dehydrogenation process, which, in turn, suggests base-induced oxidative dehydrogenation in **2**/**3**.[6] Remarkably, complexation of the PA derivative with a suitably placed electrophilic moiety in its backbone such as 4-[(pyridin-2-ylmethyl)amino]pent-3-en-2-one (**HL4**) under similar reaction conditions leads to intramolecular 5-*exo*-*trig* ring cyclization to yield a pyridylpyrrole (**L4′**) derivative in $[Ru^{II}(H)(L4')(CO)(PPh_3)_2]$ (**4**). The influence of π-accepting CO/PPh_3 facilitates stabilization of the Ru^{II} state in **1**−**4** (Scheme 2).

Replacement of the electron-withdrawing pyridine ring of PA in **HL4** by the electron-donating thiophene ring in [(thiophen-2-ylmethyl)amino]pent-3-en-2-one (**HL5**) yields ruthenium-coordinated **L5**$^-$ in $[Ru^{II}(H)(L5)(CO)(PPh_3)_2]$ (**5**) instead of the otherwise expected five-membered metallaheterocycle as in **4** (Scheme 2). It indeed signifies the pivotal role of the pyridinyl moiety and Lewis acidity of the transition metal in the ring-closing process.

In contrast, the introduction of a bulkier "Ph" group at the C_α position (**HL6**) inhibits the aforestated ring formation on the $[Ru(Cl)(H)(CO)(PPh_3)_3]$ platform (Scheme 2) because of the improper orientation of the linking atoms to achieve the optimal trajectory, as has also been revealed from its crystal structure (Figure 1). It, however, affords metal acetylacetonate (**6**) and phenyl(pyridin-2-yl)methanimine along with ill-defined side products as a consequence of the *N*-dealkylation process. A similar phenomenon has also been observed for the analogous **HL7** bearing methyl substitution at C_α. The formation of a phenyl(pyridin-2-yl)methanimine or (pyridin-2-yl)ethanimine byproduct during the reaction of $[Ru(Cl)(H)(CO)(PPh_3)_3]$ and **HL6** or **HL7**, respectively, is supported by the respective gas chromatography (GC)−mass spectrometry (MS) spectra.

The impact of an electron-poor $\{Ru^{II}(H)(CO)(PPh_3)_2\}$ metal fragment toward the ring cyclization process in **4** has been further verified by considering an alternate metal precursor, $\{Ru^{II}(pap)_2\}$, encompassing strongly π-accepting pap = 2-phenylazopyridine[7] (Scheme 3). As anticipated, the reaction proceeds through the same ring-closing process to yield $\{Ru^{II}(pap)_2\}$-chelated pyridylpyrrole (**L4′**) in **4A**, supported by its mass/NMR (Figures S1 and S12).

The ligands and complexes have been characterized by their crystal structures, electrospray ionization mass spectrometry (ESI-MS)/GC−MS, and spectroscopic ($^1H/^{13}C/^{31}P$ NMR, UV−vis, and IR) signatures (Figure 1, Table 1, and Figures S1−S16 and Tables S1−S7). N,N and O,O donors of the functionalized PA (i.e., L′) form five- and six-membered chelates with the metal ions in **1**−**4** and **6**, respectively (Figure 1). The anionic N2 donor of **L1′** (**1**) or **L4′** (**4**) is in a *trans* orientation with respect to the M−CO bond because of the *trans* effect of CO. A comparison of the Ru1−C1(CO) and C1−O1 bonds in **1** and **4** suggests a lesser synergistic back-bonding effect [$(d\pi)Ru^{II} \rightarrow (\pi^*)CO$; M−C≡O ↔ M=C=O] in the latter[8] because of electron delocalization from the pyrrolide moiety to the pyridyl backbone in **L4′**, as has also been reflected in its remarkably shorter C6−C7 bond length [1.411(8) Å]. Consequently, the amidate function of the carboxamido ligand (**L1′**) in **1** is perturbed to some extent, as supported by its partially biased C7=O2 [1.26(1) Å] and C7−N2 [1.35(1) Å] distances.[9] In contrast, CO remains *trans* to the pyridyl or isoquinolyl N1 in **2** or **3** incorporating two

DOI: 10.1021/acs.inorgchem.9b03065
Inorg. Chem. XXXX, XXX, XXX−XXX

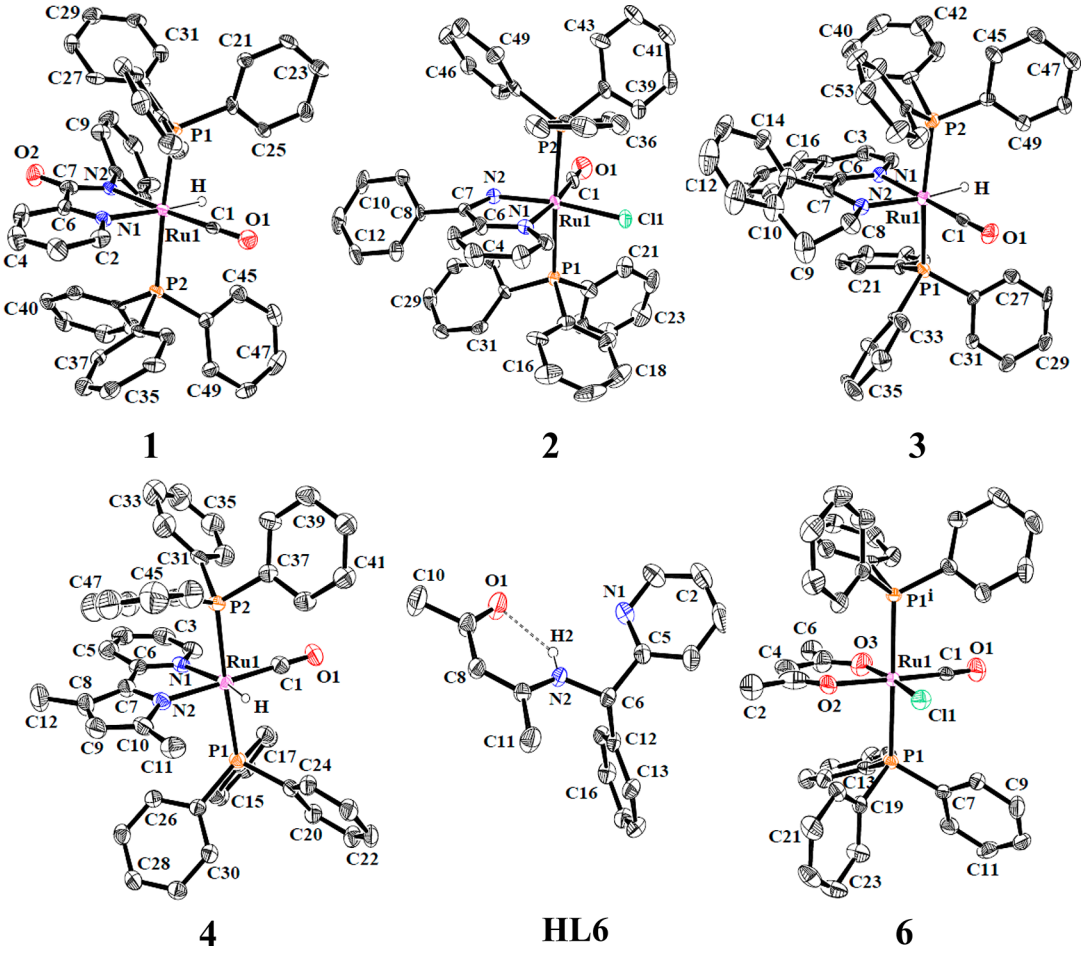

Figure 1. ORTEP diagrams. H atoms (except the selective one), solvent molecules, and counteranions are omitted for clarity. Thermal ellipsoids are at 40% probability.

Scheme 3. Impact of the Ancillary Ligand on Cyclization

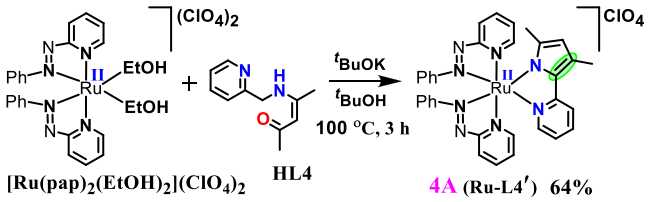

Table 1. Selected Crystallographic Bond Lengths (Å)

	1	2	3	4
Ru1−C1	1.822(7)	1.86(1)	1.847(9)	1.860(5)
C1−O1	1.185(9)	1.11(2)	1.16(1)	1.136(6)
C7−N2	1.35(1)	1.29(1)	1.31(1)	1.373(8)
C6−C7	1.51(1)	1.48(2)	1.48(1)	1.411(8)
C6−N1	1.353(9)	1.39(1)	1.329(9)	1.379(6)

neutral N donors, respectively. This causes a lesser extent of Ru1−C1 or C1−O1 bond perturbation. The appearance of a new C7═O2 bond in **L1′** of **1** and the disappearance of the C═O bond of the *β*-ketoiminate (acnac) fragment in **L4′** of **4** are attributed to functionalization of the picolyl (C7) center, as has also been supported by their NMR resonances. On the other hand, dehydrogenation of amine → imine in **2**/**3** is evident from the shorter C7−N2 bond length in **L2′**/**L3′** as well as by the absence of the picolyl proton (C_α−H) in ^{1}H NMR. Each complex molecule displays one ^{31}P NMR signal corresponding to two *trans*-positioned PPh_3 groups and a triplet pattern for Ru−H of **1**, **3**, and **4** in ^{31}P NMR due to its coupling with two PPh_3 ($\Sigma I = 1$) groups.[10]

Effect of External Electrophiles. In order to understand the role of external electrophiles, the reaction of **HL1** and $[Ru(Cl)(H)(CO)(PPh_3)_3]$ is carried out in the presence of benzyl bromide (an external electrophile) and ^{t}BuOK base in dry toluene under an inert atmosphere. It yields metal-coordinated imine in $[Ru(\mathbf{L1''})(Br)_2(CO)PPh_3]$ (**1A**) instead of the insertion of an electrophile ($-CH_2Ph$) at the C_α position of PA (Figures 2a and S13). Excess benzyl bromide in the reaction has possibly played the dual role of substrate and oxidant. Moreover, the formation of **1A** is associated with the additional ligand-exchange processes, i.e., initial labilization of bulky PPh_3 by a bromide ion followed by the consequent substitution of other anionic ligands. Further, the base-induced rapid dehydrogenation process of PA under an inert atmosphere did not allow intermolecular reaction between the external electrophile and nucleophilic methylene center of PA.

The analogous reaction of $[Ru(Cl)(H)(CO)(PPh_3)_3]$ and **HL2** in the presence of methylene iodide in lieu of benzyl bromide as an external electrophile results in **2** (imine product, major) along with a metal-coordinated amine product in $[Ru(I)_2(CO)(\mathbf{L2})(PPh_3)_2]$ (**2A**, minor; Figure 2b). The decrease in the Lewis acidity of the metal ion in the presence

DOI: 10.1021/acs.inorgchem.9b03065
Inorg. Chem. XXXX, XXX, XXX−XXX

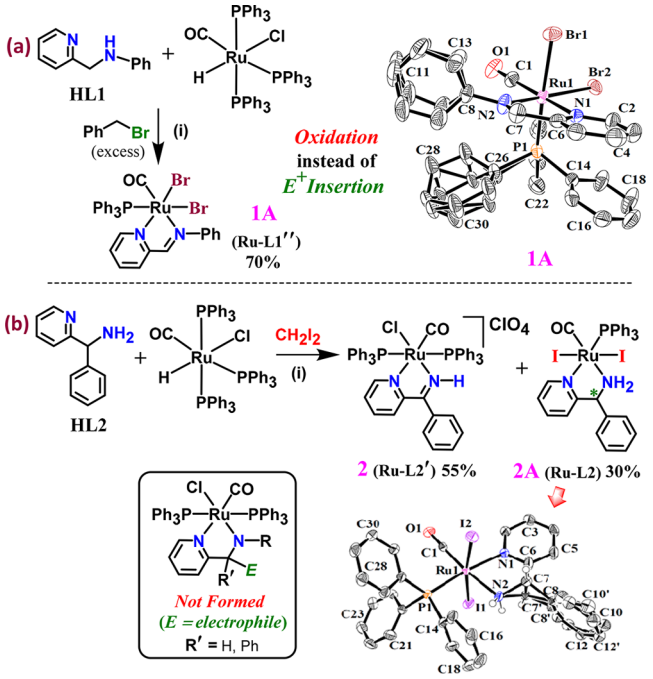

Figure 2. Reaction with external electrophiles. Reaction conditions: (i) ^{t}BuOH/^{t}BuOK, N_2 atmosphere, 100 °C, 12 h. (a) Imine formation under an inert atmosphere. ORTEP of **1A**. Bond lengths (Å): C7−N2 1.287(8); C6−C7, 1.459(8); C6−N1, 1.341(6). (b) Ligand-exchange reaction. ORTEP of **2A**. Bond lengths (Å): C7−N2, 1.499(7); C6−C7, 1.603(8); C6−N1, 1.336(5).

of a weak-field iodide ligand possibly facilitates stabilization of the metalated amine in **2A**. The simultaneous formation of **2** and **2A** rationalizes a competitive scenario, C−H activation versus ligand-exchange phenomenon at the metal center in inhibiting the desired functionalization.

Mechanistic Outline. To gain insights into the aforesaid transformation processes, a controlled reaction involving **HL2** with a phenyl substituent at its C_α and [Ru(Cl)(H)(CO)-$(PPh_3)_3$] has been followed in refluxing dry toluene in the presence of ^{t}BuOK under anoxic conditions. The resultant green solution, however, quickly changes to **2** (yellow) under oxic conditions. The transformation of green to yellow (**2**) is monitored spectrophotometrically in deaerated tetrahydrofuran (THF) at 313 K (Figure 3). ^{1}H NMR of the in situ generated green solution in benzene-d^6 fails to display the characteristic resonance of C_α−H around 3−5.5 ppm (Figure S5f), possibly implying involvement of the dianionic intermediate (**DA**, Figure 4) in the conversion sequence.[11,5a] **DA_2** (Figure 4) was selectively chosen to follow because phenyl substitution at the methine carbon of **HL2** has

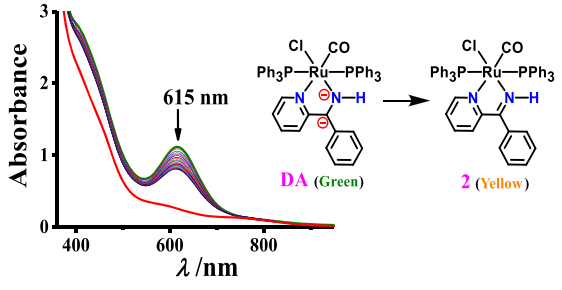

Figure 3. Change in the spectral profile for **DA** → **2** in THF at 313 K.

extended additional stability to the system via conjugation of C_α^- (**DA_2**) into the phenyl ring along with the pyridyl moiety.

Therefore, a common dianionic intermediate (**DA**), generated via activation of the acidic methylene group of PA upon coordination to electrophilic {Ru(H/Cl)(CO)$(PPh_3)_2$} or {Ru$(pap)_2$}, is considered to correlate the reactivity patterns.[11,5a] The reactive C_α center of **DA_1** (no longer "spectator") reacts with the molecular oxygen in an intermolecular fashion to yield **1**. However, the presence of an electrophilic substituent at **DA_4** facilitates the intramolecular reaction between the carbonyl center and reactive C_ω leading to the formation of a cyclized product in **4**. On the contrary, substitution at C_α results in imine (**2** or **3**) via two-electron oxidation of **$DA_{2/3}$**. Similarly, the formation of imine in **1A** (Figure 2a) can be attributed to two-electron oxidation of in situ generated **DA_1** (Figure 4) under anoxic conditions. The apparently unfavorable formation of **DA** encompassing two adjacent negative charges (Figure 4) could possibly be stabilized to some extent by π-back-donation from $Ru^{II}(t_{2g}^6)$ to CO/PPh_3 as well as via the delocalization of negative charge into the pyridine moiety to form a dearomatized structure, as depicted in Figure 4.[8,12] Thus, the cooperative interplay of metal chelation and suitable substituents in the PA frameworks is decisive for the substrate activation processes. Further, in the present scenario, PA with a suitably positioned electrophilic function (as in **HL4**, Scheme 2) follows the faster *intramolecular* cyclization path (**4** in Scheme 2) instead of the *intermolecular* oxygenation route.

The proposed pathway in Figure 4 has further been evaluated computationally by using the B3LYP/6-31G**/LANL2DZ level of theory (Figures 5 and S17−S19 and Table S8).[13] The outline of the oxygenation process in Figure 4 is derived primarily based on the earlier reports by de Bruin and co-workers for the analogous system.[5a,14] The first step for the oxygenation process through the anionic pathway involves the formation of a short-lived peroxide intermediate (**$I1_{1a}$** in Figure 5; O−O = 1.465 Å), which undergoes subsequent proton shuttling (**TS_{1a}**) followed by heterolytic cleavage of the O−O bond to generate thermodynamically stable **1**. The formation of a peroxide intermediate has been considered to follow via either (i) one-electron oxidation of **DA_1** ({Ru^{II}-**$L1^{2-}$**}$^-$, $S = 0$) by molecular oxygen ($^3O_2$, $S = 1$) to produce **$DA_1^\bullet$** ({Ru^{II}-**$L1^{\bullet-}$**}, $S = {}^1/_2$) and $O_2^{\bullet-}$ ($S = {}^1/_2$), followed by their intermolecular interaction, or (ii) interaction of **DA_1** ($S = 0$) with $^1O_2$ ($S = 0$). The necessary change in the multiplicities for the activation of $^3O_2(^3\Sigma_g^-)$ to $^1O_2(^1\Delta_g)$ in pathway ii may be assisted by its interaction with the complex under a strong crystal field.[15,16] The density functional theory (DFT) calculations, however, prefer pathway i over pathway ii [ΔE(path ii−path i) = ∼33 kcal mol^{-1}]. Nevertheless, the presence of K^+ provides further stability to the system (Figure S18). The selective interaction of a π_g^* singly occupied molecular orbital of superoxide with the methine center of **$DA_1^\bullet$** in pathway i has also been supported by the **L1**-dominated spin in **$DA_1^\bullet$** (**L1**, 0.99; {Ru(H)(CO)$(PPh_3)_2$}, 0.01; Figure S19).

The alternate radical pathway (Figure 4) involving the interaction of in situ generated one-electron-oxidized **$DA_1^\bullet$** ($S = {}^1/_2$) with ground-state $^3O_2$ (diradical, $S = 1$) is also equally probable.[5a,14] This gives rise to the oxygenated **L1′** in **1** via a possible superoxide intermediate ($S = {}^1/_2$).[17] Electron release and uptake processes are, however, balanced in the reaction sequence.

DOI: 10.1021/acs.inorgchem.9b03065
Inorg. Chem. XXXX, XXX, XXX−XXX

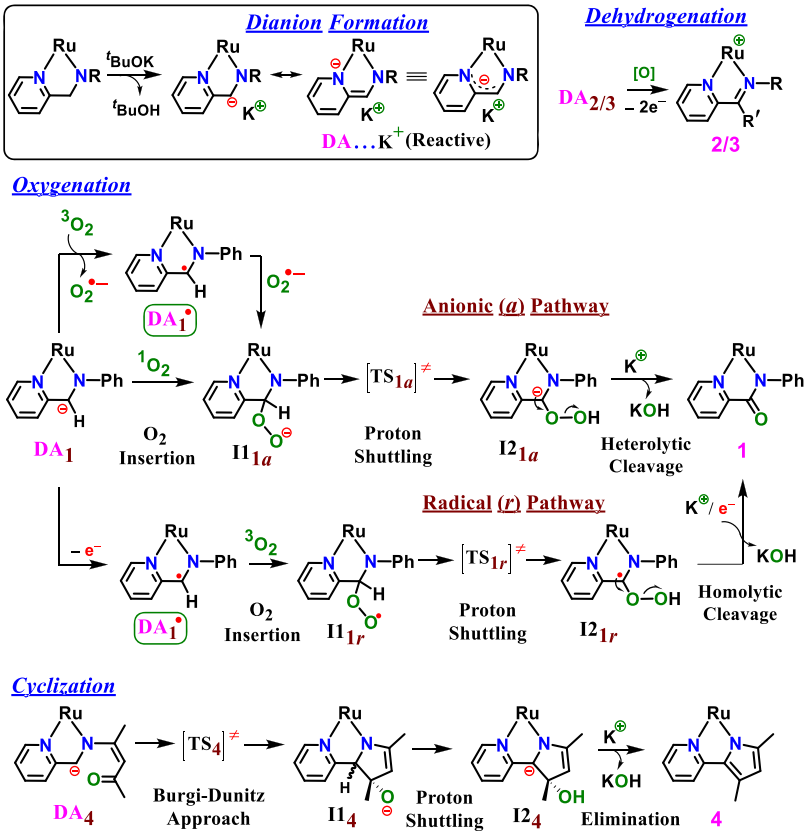

Figure 4. Proposed pathway for correlation of the reactivities. Charge on the amide nitrogen (N^-) is not shown for clarity. *a* stands for the anionic pathway, and *r* stands for the radical pathway.

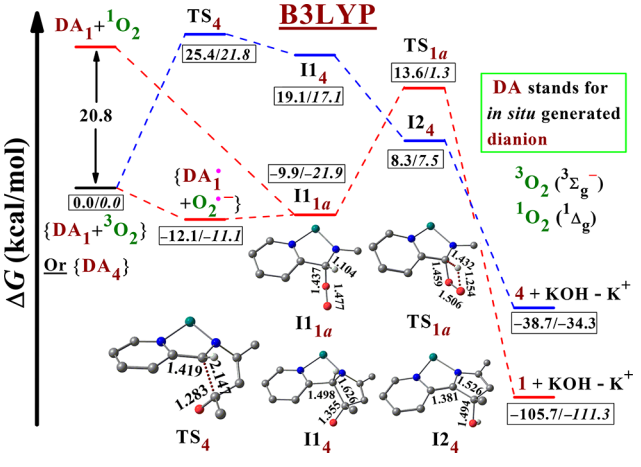

Figure 5. Gibbs free energy (ΔG, 298 K) profile (not to scale) for the formation of **1** (anionic pathway, red) and **4** (blue) at the B3LYP level in 2-butanol.[13] The associated $\Delta G/\Delta H$ are shown in each state. ΔG of the starting substrates is taken as zero. Only the core structures are shown here.

The reaction pathway for **4** includes a 5-*exo*-*trig* cyclization between anionic C_α and electrophilic C═O counterparts of the acnac moiety. The approach of in situ generated C_α^- to the carbonyl moiety (S_N^2 path) at an angle of 112° (close to the Burgi–Dunitz angle, $\mathbf{TS_4}$ in Figure 5) extends the optimum trajectory for $n(C_\alpha^-) \rightarrow \pi^*(C{=}O)$ interaction.[18] This leads to transient $\mathbf{I1_4}$, which then rearranges to $\mathbf{I2_4}$. The lowering in energy of $\mathbf{I2_4}$ may be a consequence of the negative charge delocalization onto the pyridyl backbone. Elimination of KOH at the final stage directs the formation of **4**. Elongation of a newly formed C–C bond in $\mathbf{I1_4}$ (>1.6 Å) and a C–O distance in $\mathbf{I2_4}$ (1.493 Å) is a reflection of electronic consequence due to molecular strain.[19] Moreover, cyclization in the presence of an acnac substituent in PA also reveals the ambiphilic feature of acnac.[20] Finally, the greater thermodynamic stability of the products (ΔG highly negative) with respect to their metastable dianionic counterpart favors the overall transformation processes.

CONCLUSION

Although PA-derived ligands have widely been applied as "spectator" ligands, the present paper highlights a diverse reactivity profile (aerobic oxygenation, dehydrogenation, ring formation, and *N*-dealkylation) of suitably designed PA derivatives (i.e., their "chemical noninnocence") on selective ruthenium platforms. Correlation of the reactivity suggests that simple tuning of the PA backbone at the amine nitrogen results in its varying functionalization modes including intermolecular (oxygenation) to intramolecular (cyclization) transformations. On the other hand, insertion of an alkyl or aryl sustituent at the C_α of PA inhibits the aforestated conversions and instead facilitates the dehydrogenation or *N*-dealkylation process. The present deliberation is therefore expected to introduce a new avenue in the specific direction of metal-assisted C–H functionalization to achieve biologically relevant heterocyclic ring congeners via fine tuning of the ligand environment.

EXPERIMENTAL SECTION

Materials. The precursor complexes $[Ru(Cl)(H)(CO)(PPh_3)_3]$[21] and *ctc*-$[Ru(pap)_2(EtOH)_2]$[22] and the ligands **HL1**–**HL4**[23−26] were

DOI: 10.1021/acs.inorgchem.9b03065
Inorg. Chem. XXXX, XXX, XXX–XXX

prepared by following the literature procedures. Newly designed **HL5**−**HL7** were synthesized by following a procedure similar to that for **HL4**.[26] Other chemicals and solvents were of reagent grade and were used as received. For spectroscopic studies, HPLC-grade solvents were used. $^{18}O_2$ was procured from ICON Isotope.

Physical Measurements. The electrical conductivity was checked using an autoranging conductivity meter (Toshcon Industries, India). $^{1}H/^{13}C$/DEPT-135/^{31}P NMR spectra were recorded on a Bruker Avance III 400 or 500 MHz spectrometer. Elemental analyses were recorded on a Thermoquest (EA 1112) microanalyzer or a Thermo Finnigan (FLASH EA 1112) instrument. The ESI-MS was checked on a Bruker Maxis Impact (282001.00081) spectrometer. GC−MS experiments were performed on an Agilent 5975C spectrometer. IR spectra of the complexes were recorded on a Nicolet spectrophotometer. Electronic spectral studies were performed on a PerkinElmer Lambda 1050 spectrophotometer.

Crystallography. X-ray diffraction data were collected using a Rigaku Saturn-724+ CCD single-crystal X-ray diffractometer using a Mo Kα or Cu Kα source. Data collection was evaluated by using the *Crystal Clear-SM Expert* software. The data were collected by the standard ω-scan technique. The structures were solved by direct methods using *SHELXS-97* and refined on F^2 by full matrix least squares with *SHELXL-2014/2016/2018*.[27] All data were corrected for Lorentz and polarization effects, and all non-H atoms were refined anisotropically. The remaining H atoms were placed in geometrically constrained positions and refined with isotropic temperature factors, generally 1.2U_{eq} of their parent atoms. H atoms were included in the refinement process as per the riding model. CCDC 1951286 (**1**), 1951287 (**2**), 1951288 (**3**), 1951290 (**4**), 1951289 (**6**), 1951291 (**1A**), 1951292 (**2A**), and 1951293 (**HL6**) contain the supplementary crystallographic data for this paper. These data can be obtained free of charge from The Cambridge Crystallographic Data Centre via www.ccdc.cam.ac.uk/data_request/cif.

Computational Studies. Full geometry optimization was performed by using the DFT method at the B3LYP level.[28] Except ruthenium, all other elements were assigned the 6-31G** basis set. The LANL2DZ basis set with an effective core potential was employed for the Ru atom.[29] All calculations were performed with the *Gaussian 09* program package.[30] Calculated structures were visualized with *ChemCraft*.[31]

Transition-state calculations were performed at the B3LYP level of theory starting from infinitely separated substrates. Single imaginary frequencies for the transition states (TSs) and real frequencies for the local minima were obtained. The connectivity of each TS was validated through a relaxed potential energy surface scan for the corresponding reaction coordinate and found to be the highest-energy point that connected the relevant reactant and product. The zero-point vibrational energies and thermal corrections were obtained from the harmonic frequency calculations at the B3LYP level of theory in 2-butanol.

*General Procedure for the Synthesis of **HL5**−**HL7**.* Acetylacetone was added dropwise to a methanolic solution of the respective amines, and the mixture was stirred overnight under refluxing conditions to obtain a yellow solution. It was washed with *n*-pentane and dried under vacuum. Purification by column chromatography (using a neutral alumina column with a varying ratio of the dichloromethane/acetonitrile mixture) led to the resulting yellow oily liquid of the corresponding **HL**.

*4-[(Thiophen-2-ylmethyl)amino]pent-3-en-2-one (**HL5**).* Thiophen-2-ylmethanamine (5.0 mL, 48.7 mmol) and acetylacetone (5.0 mL, 48.7 mmol) were used. Yield: 8.5 g (90%). ^{1}H NMR (500 MHz, $CDCl_3$): δ 11.07 (s, 1H), 7.18 (dd, 1H), 6.91 (s, 1H), 5.01 (s, 1H), 4.55 (d, J = 6.1 Hz, 2H), 1.99 (s, 3H), 1.93 (s, 3H). ^{13}C NMR (126 MHz, $CDCl_3$): δ 195.51, 162.43, 141.21, 127.02, 125.05, 124.91, 96.21, 41.89, 28.91, 18.75. DEPT-135 (126 MHz, $CDCl_3$): δ 127.02, 125.05, 124.91, 96.21, 41.90, 28.91, 18.76. HRMS ($C_{10}H_{13}NOS$; {**HL5** + H}$^+$). Calcd: m/z 196.0791. Found: m/z 196.0786. IR: 1647 cm^{-1} [ν(C═O)].

*4-[[Phenyl(pyridin-2-yl)methyl]amino]pent-3-en-2-one (**HL6**).* Phenyl(pyridin-2-yl)methanamine (5.0 g, 27.1 mmol) and acetylacetone (2.7 mL, 27.1 mmol) were used. Yield: 5.6 g (78%). Single crystals of **HL6** were obtained from a 2:1 dichloromethane/methanol solution. ^{1}H NMR (400 MHz, $CDCl_3$): δ 8.51 (d, J = 4.1 Hz, 1H), 7.52 (td, J = 7.7 and 1.6 Hz, 1H), 7.33 (d, J = 7.5 Hz, 2H), 7.24 (t, J = 7.7 Hz, 3H), 7.15 (t, J = 7.3 Hz, 1H), 7.07−7.01 (m, 1H), 5.79 (d, J = 7.9 Hz, 1H), 5.01 (s, 1H), 1.99 (s, 3H), 1.81 (s, 3H). ^{13}C NMR (101 MHz, $CDCl_3$): δ 195.63, 161.86, 160.29, 149.49, 141.22, 137.12, 128.95, 127.70, 126.77, 122.45, 121.12, 96.65, 62.99, 28.96, 19.41. DEPT-135 (101 MHz, $CDCl_3$): δ 149.49, 137.12, 128.95, 127.70, 126.77, 122.44, 121.12, 96.65, 62.99, 28.96, 19.40. HRMS ($C_{17}H_{18}N_2O$; {**HL6** + H}$^+$). Calcd: m/z 267.1492. Found: m/z 267.1477. IR: 1603 cm^{-1} [ν(C═O)].

*4-[[1-(Pyridin-2-yl)ethyl]amino]pent-3-en-2-one (**HL7**).* 1-(Pyridin-2-yl)ethan-1-amine (5.0 mL, 41.0 mmol) and acetylacetone (4.2 mL, 41.0 mmol) were used. Yield: 7.2 g (86%). ^{1}H NMR (500 MHz, $CDCl_3$): δ 11.19 (d, J = 6.7 Hz, 1H), 8.48 (dt, J = 1.5 and 4.5 Hz, 1H), 7.61 (td, J = 7.7 and 1.8 Hz, 1H), 7.22 (d, J = 7.9 Hz, 1H), 7.11 (ddd, J = 7.5, 4.9, and 1.1 Hz, 1H), 4.95 (s, 1H), 4.77−4.69 (m, 1H), 1.97 (s, 3H), 1.75 (s, 3H), 1.51 (s, 3H). ^{13}C NMR (126 MHz, $CDCl_3$): δ 195.48, 162.90, 162.35, 149.20, 137.24, 122.22, 119.52, 96.03, 54.72, 28.88, 23.05, 19.16. DEPT-135 (126 MHz, $CDCl_3$): δ 149.20, 137.24, 122.21, 119.52, 96.03, 54.72, 28.88, 23.05, 19.16. HRMS ($C_{12}H_{16}N_2O$; {**HL7** + H}$^+$). Calcd: m/z 205.1335. Found: m/z 205.1344. IR: 1610 cm^{-1} [ν(C═O)].

Preparation of the Complexes. *Synthesis of **1**−**5**.* Complexes **1**−**5** were prepared by following a general synthetic route using the respective preformed HL ligands. To the pale-pink solution of [Ru(Cl)(H)(CO)(PPh_3)$_3$] in ^{t}BuOH in an oven-dried round bottom flask was added a yellow solution of the respective **HL** in ^{t}BuOH and ^{t}BuOK. The solution was refluxed under an aerial atmosphere for ∼4 h. The solution gradually turned to yellow with progression of the reaction. Evaporation of the solvent under vacuum afforded a yellow solid, which was subjected to chromatographic purification by using a neutral alumina column and varying the mixture of dichloromethane/petroleum ether as the eluent. Removal of the solvent under vacuum resulted in complexes **1**−**5**. An aqueous solution of excess $NaClO_4$ was added to precipitate the cationic complexes **2** and **3**.

*[Ru^{II}(H)(**L1′**)(CO)(PPh_3)$_2$] (**1**).* [Ru(Cl)(H)(CO)(PPh_3)$_3$] (150 mg, 0.158 mmol), **HL1** (29 mg, 0.158 mmol), ^{t}BuOH (20 mL), ^{t}BuOK (53 mg, 0.473 mmol). Yield: 118 mg (88%). Slow evaporation of its dichloromethane solution gave yellow crystals of **1**. MS (ESI$^+$, CH_3CN; {**1**}$^+$). Calcd: m/z 851.16. Found: m/z 851.18. ^{1}H NMR (500 MHz, $CDCl_3$): δ 7.92 (d, J = 5.1 Hz, 1H), 7.73 (d, J = 7.8 Hz, 1H), 7.71−7.63 (m, 2H), 7.60−7.52 (m, 2H), 7.46 (td, J = 7.5 and 2.6 Hz, 3H), 7.44−7.33 (m, 11H), 7.22 (t, J = 7.3 Hz, 6H), 7.15 (t, J = 7.3 Hz, 10H), 6.96−6.88 (m, 2H), 6.63−6.57 (m, 2H), −10.43 to −10.66 (t, 1H). ^{13}C NMR (126 MHz, $CDCl_3$): δ 206.30, 166.00, 158.15, 153.46, 150.82, 133.72, 133.66, 133.60, 129.28, 128.03, 127.99, 127.94, 127.25, 127.08, 126.16, 125.46, 124.08, 121.47. ^{31}P NMR (162 MHz, $CDCl_3$): δ 43.43. Anal. Calcd for $C_{49}H_{40}N_2O_2P_2Ru$: C, 69.09; H, 4.73; N, 3.29. Found: C, 69.37; H, 4.57; N, 3.34. IR (KBr, cm^{-1}): 1919 [ν(C≡O)], 1664 [ν(C═O)$_{PA}$]. Molar conductivity (CH_3CN): Λ_M = 6 Ω^{-1} cm^2 M^{-1}. UV−vis [λ, nm (ε, M^{-1} cm^{-1})]: 338 (5200), 233 (38200).

*[Ru^{II}(Cl)(**L2′**)(CO)(PPh_3)$_2$]ClO_4 (**2**).* [Ru(Cl)(H)(CO)(PPh_3)$_3$] (150 mg, 0.158 mmol), **HL2** (29 mg, 0.158 mmol), $NaClO_4$(190 mg, 1.58 mmol, 10 equiv), ^{t}BuOH (20 mL), and ^{t}BuOK (53 mg, 0.473 mmol) were used. Yield: 116 mg (76%). Slow evaporation of its dichloromethane solution gave reddish-yellow crystals of **2**. MS (ESI$^+$, CH_3CN; {**2** − ClO_4}$^+$). Calcd: m/z 871.13. Found: m/z 871.17. ^{1}H NMR (400 MHz, CD_3CN): δ 10.91 (s, 1H), 7.91 (t, J = 7.8 Hz, 1H), 7.83 (d, J = 5.1 Hz, 1H), 7.59 (d, J = 7.7 Hz, 1H), 7.51 (t, J = 7.6 Hz, 2H), 7.43 (dd, J = 11.4 and 5.0 Hz, 8H), 7.39−7.25 (m, 24H), 7.05−7.00 (m, 1H), 6.34 (d, J = 7.2 Hz, 2H). ^{13}C NMR (101 MHz, CD_3CN): δ 203.89, 177.25, 151.72, 151.13, 138.87, 133.86, 133.80, 133.75, 132.61, 131.48, 130.85, 129.85, 129.74, 129.51, 129.28, 128.82, 128.77, 128.72, 128.65, 127.44, 117.37. ^{31}P NMR (162 MHz, $CDCl_3$): δ 37.43. Anal. Calcd for $C_{49}H_{40}N_2O_5P_2Cl_2Ru$: C, 60.62; H, 4.15; N, 2.89. Found: C, 60.95; H, 4.13; N, 2.63. IR (KBr, cm^{-1}): 1977 [ν(C≡O)]. Molar conductivity (CH_3CN): Λ_M = 102 Ω^{-1} cm^2

DOI: 10.1021/acs.inorgchem.9b03065
Inorg. Chem. XXXX, XXX, XXX−XXX

M^{-1}. UV−vis [λ, nm (ε, M^{-1} cm^{-1})]: 440 (800), 281 (10400), 238 (10600).

*[Ru^{II}(H)(**L3′**)(CO)(PPh$_3$)$_2$]ClO$_4$ (**3**).* [Ru(Cl)(H)(CO)(PPh$_3$)$_3$] (150 mg, 0.158 mmol), **HL3** (41 mg, 0.158 mmol), NaClO$_4$(190 mg, 1.58 mmol, 10 equiv), ^{t}BuOH (20 mL), and ^{t}BuOK (53 mg, 0.473 mmol) were used. Yield: 132 mg (83%). Slow evaporation of its 2:1 dichloromethane/hexane solution gave crystals of **3**. MS (ESI$^+$, CH_3CN; {**3** − ClO_4}$^+$). Calcd: m/z 913.21. Found: m/z 913.17. ^{1}H NMR (400 MHz, $CDCl_3$): δ 8.79 (d, J = 5.9 Hz, 1H), 8.0−6.5 (m, 39H), 4.49 (d, J = 16.0 Hz, 1H), 2.95 (t, J = 16.2 Hz, 1H), 2.65 (d, J = 17.6 Hz, 1H), 2.41−2.25 (m, 1H), −10.67 (t, J = 20.2 Hz, 1H). ^{13}C NMR (101 MHz, $CDCl_3$): δ 204.01, 166.55, 154.16, 153.78, 152.31, 146.25, 146.17, 145.91, 137.06, 136.51, 136.01, 133.23, 133.17, 132.11, 132.06, 131.94, 130.67, 130.50, 130.34, 128.68, 128.64, 128.46, 128.41, 127.85, 127.57, 125.59, 124.75, 116.91, 56.39, 27.28. DEPT-135 (^{13}C NMR; 101 MHz, $CDCl_3$): δ 145.91, 133.17, 133.04, 132.12, 130.67, 130.50, 130.34, 128.64, 128.29, 127.85, 127.57, 127.20, 126.38, 126.10, 125.60, 124.75, 56.32, 27.27. ^{31}P NMR (202 MHz, $CDCl_3$): δ 43.70. IR (KBr, cm^{-1}): 1972 [ν(C≡O)]. Anal. Calcd for $C_{55}H_{45}N_2O_5P_2Cl_1Ru$: C, 65.25; H, 4.48; N, 2.77. Found: C, 65.57; H, 4.73; N, 2.47. Molar conductivity (CH_3CN): Λ_M = 94 Ω^{-1} cm^2 M^{-1}. UV−vis [λ, nm (ε, M^{-1} cm^{-1})]: 496 (4880), 388 (15820).

*[Ru^{II}(H)(**L4′**)(CO)(PPh$_3$)$_2$] (**4**).* [Ru(Cl)(H)(CO)(PPh$_3$)$_3$] (150 mg, 0.158 mmol), **HL4** (30 mg, 0.158 mmol), ^{t}BuOH (20 mL), and ^{t}BuOK (53 mg, 0.473 mmol) were used. Yield: 120 mg (93%). Slow evaporation of its 2:1 dichloromethane/hexane solution gave crystals of **4**. MS (ESI$^+$, CH_3CN; {**4** + H}$^+$). Calcd: m/z 827.19. Found: m/z 827.20. ^{1}H NMR (500 MHz, $CDCl_3$): δ 7.40−7.32 (m, 12H), 7.30−7.25 (t, J = 7.3 Hz, 7H), 7.24−7.16 (t, J = 7.5 Hz, 15H), 5.85 (s, 1H), 2.31 (s, 3H), 1.60 (s, 3H), −10.52 to −10.65 (t, J = 20.8 Hz, 1H). ^{13}C NMR (101 MHz, $CDCl_3$): δ 156.51, 152.07, 141.33, 134.12, 133.99, 133.93, 133.87, 133.71, 133.60, 128.87, 127.60, 127.56, 127.51, 124.13, 115.37, 114.22, 114.06, 16.92, 14.90. ^{31}P NMR (162 MHz, $CDCl_3$): δ 44.85. Anal. Calcd for $C_{48}H_{42}N_2OP_2Ru$: C, 69.81; H, 5.13; N, 3.39. Found: C, 69.32; H, 5.36; N, 3.52. IR (KBr, cm^{-1}): 1913 [ν(C≡O)]. Molar conductivity (CH_3CN): Λ_M= 2 Ω^{-1} cm^2 M^{-1}. UV−vis [λ, nm (ε, M^{-1} cm^{-1})]: 408(sh), 354 (14600), 231 (48000).

*[Ru^{II}(H)(**L5**)(CO)(PPh$_3$)$_2$] (**5**).* [Ru(Cl)(H)(CO)(PPh$_3$)$_3$] (150 mg, 0.158 mmol), **HL5** (31 mg, 0.158 mmol), ^{t}BuOH (20 mL), and ^{t}BuOK (53 mg, 0.473 mmol) were used. Yield: 13 mg (10%). The poor yield and unstable feature of **5** (possibly due to a weakly coordinating thiophenyl S donor) kept us from performing a detailed characterization except MS identification. MS (ESI$^+$, CH_3CN; {**5** − Cl}$^+$). Calcd: m/z 848.18. Found: m/z 848.17.

*Synthesis of [Ru(acac)(Cl)(CO)(PPh$_3$)$_2$] (**6**; acac = Acetylacetonate).* To a pale-pink solution of [Ru(Cl)(H)(CO)(PPh$_3$)$_3$] (150 mg, 0.158 mmol) in ^{t}BuOH (20 mL) in an oven-dried clean round-bottom flask were added a yellow solution of **HL6** (42 mg, 0.158 mmol) or **HL7** (32 mg, 0.158 mmol) in ^{t}BuOH and ^{t}BuOK (53 mg, 0.473 mmol). The solution was refluxed under an aerial atmosphere for ∼4 h. The solution gradually turned to yellow with progression of the reaction. Evaporation of the solvent under vacuum afforded a yellow solid, which was subjected to chromatographic purification by using a neutral alumina column and 1:3 dichloromethane/petroleum ether as the eluent. Removal of the solvent under vacuum resulted in complex **6**. Yield: ∼70 mg (∼55%). Slow evaporation of its 3:1 dichloromethane/methanol solution gave colorless crystals of **6**. MS (ESI$^+$, CH_3CN; {**6**}$^+$). Calcd: m/z 789.11. Found: m/z 789.15. ^{1}H NMR (400 MHz, $CDCl_3$): δ 7.79 (t, J = 6.2 Hz, 3H), 7.73−7.63 (m, 21H), 7.44−7.28 (m, 10H), 1.63 (s, 3H). ^{13}C NMR (101 MHz, $CDCl_3$): δ 193.93, 155.08, 148.59, 137.12, 136.29, 134.67, 134.61, 134.39, 133.90, 133.65, 132.97, 131.01, 129.59, 128.75, 128.49, 128.29, 128.20, 127.90, 126.24, 124.65, 94.53, 29.72, 27.15. ^{31}P NMR (162 MHz, $CDCl_3$): δ 50.94. Anal. Calcd for $C_{42}H_{37}ClO_3P_2Ru$: C, 64.00; H, 4.73. Found: C, 63.83; H, 4.93. IR (KBr, cm^{-1}): 1937 [ν(C≡O)], 1589 [ν(C=O)$_{acac}$]. Molar conductivity (CH_3CN): Λ_M = 6 Ω^{-1} cm^2 M^{-1}. UV−vis [λ, nm (ε, M^{-1} cm^{-1})]: 313 (6600), 241 (20000).

*Synthesis of [Ru(**L4′**)(pap)$_2$]ClO$_4$ (**4A**; pap = 2-Phenylazopyridine).* The starting complex *ctc*-[Ru(pap)$_2$Cl$_2$] (150 mg, 0.28 mmol) and AgClO$_4$ (117 mg, 0.56 mmol) were taken in EtOH (50 mL) and refluxed for 2 h. The precipitated AgCl was filtered off through a sintered-glass Gooch crucible. The filtrate was treated with **HL4** (54 mg, 0.28 mmol) and ^{t}BuOK (83 mg, 0.74 mmol), and the mixture was heated to reflux for 8 h under atmospheric conditions. The solvent was removed under reduced pressure. The residue was moistened with a few drops of CH_3CN. A saturated aqueous solution of NaClO$_4$ was added to the above concentrated solution and allowed to cool at 273 K overnight. The precipitate thus obtained was filtered, washed with chilled water to remove excess NaClO$_4$, and dried in vacuo over P_4O_{10}. The product was purified using a neutral alumina column with 1:5 petroleum ether/CH_2Cl_2 as the eluent. Yield: 132 mg (64%). MS (ESI$^+$, CH_3CN; {**4A** − ClO_4}$^+$). Calcd: m/z 639.16. Found: m/z 639.18. ^{1}H NMR (400 MHz, $CDCl_3$): δ 8.52 (d, J = 7.9 Hz, 1H), 8.46 (d, J = 8.0 Hz, 1H), 8.20 (dd, J = 7.0 and 5.7 Hz, 2H), 8.13 (dd, J = 7.8 and 1.1 Hz, 1H), 7.79−7.68 (m, 3H), 7.56 (t, J = 7.2 Hz, 1H), 7.50 (d, J = 8.2 Hz, 1H), 7.43 (d, J = 7.4 Hz, 1H), 7.39 (t, J = 6.7 Hz, 1H), 7.28−7.11 (m, 5H), 7.01 (d, J = 8.1 Hz, 2H), 6.98 (d, J = 8.2 Hz, 2H), 6.64 (t, J = 7.1 Hz, 1H), 5.78 (s, 1H), 2.42 (s, 3H), 1.54 (s, 3H). ^{13}C NMR (101 MHz, $CDCl_3$): δ 165.61, 156.46, 153.74, 149.72, 149.36, 148.87, 144.44, 139.47, 138.38, 138.03, 133.73, 133.27, 132.71, 129.43, 128.99, 128.39, 127.89, 127.76, 126.49, 123.04, 122.98, 118.47, 118.12, 116.12, 15.58, 14.15. Anal. Calcd for $C_{33}H_{29}N_8O_4Cl_1Ru$: C, 53.69; H, 3.96; N, 15.18. Found: C, 53.82; H, 3.62; N, 14.92. IR (KBr, cm^{-1}): 1214 [ν(ClO_4)]. Molar conductivity (CH_3CN): Λ_M = 106 Ω^{-1} cm^2 M^{-1}. UV−vis [λ, nm (ε, M^{-1} cm^{-1})]: 546 (5200), 331 (20600), 225(sh).

Caution! *Perchlorate salts are generally explosive and should be handled with care.*

*Synthesis of [Ru(Br)$_2$(**L1″**)(CO)(PPh$_3$)] (**1A**).* To a pale-pink solution of [Ru(Cl)(H)(CO)(PPh$_3$)$_3$] (150 mg, 0.158 mmol) in degassed toluene (20 mL) in an oven-dried Schlenk tube were added under a N_2 atmosphere **HL1** (29 mg, 0.158 mmol), followed by ^{t}BuOK (53 mg, 0.473 mmol) and benzyl bromide (95 μL, 0.80 mmol; approximately 5 equiv with respect to the ligand). The solution was refluxed under an inert atmosphere overnight. The solution gradually turned yellow with progression of the reaction. Evaporation of the solvent under vacuum afforded a yellow solid, which was subjected to chromatographic purification by using a neutral alumina column and 1:1 dichloromethane/petroleum ether as the eluent. Removal of the solvent under vacuum resulted in **1A**. Yield: 81 mg (70%). Slow evaporation of its 2:1 dichloromethane/hexane solution gave orange crystals of **1A**. MS (ESI$^+$, CH_3CN; {**1A** + H}$^+$). Calcd: m/z 734.92. Found: m/z 734.90. ^{1}H NMR (500 MHz, DMSO-d_6): δ 8.79 (d, 1H), 8.78 (s, 1H), 7.24−7.18 (m, 6H), 7.18−7.10 (m, 10H), 7.07−7.02 (m, 7H). ^{13}C NMR (126 MHz, DMSO-d_6): δ 169.31, 154.23, 152.37, 151.11, 138.96, 133.25, 133.18, 132.57, 132.18, 130.28, 129.35, 129.06, 128.76, 128.55, 128.47, 123.30. ^{31}P NMR (162 MHz, DMSO-d_6): δ 48.71. Anal. Calcd for $C_{31}H_{25}Br_2N_2OPRu$: C, 50.77; H, 3.44; N, 3.82. Found: C, 50.39; H, 3.29; N, 3.67. IR (KBr, cm^{-1}): 1969 [ν(C≡O)]. Molar conductivity (CH_3CN): Λ_M = 4 Ω^{-1} cm^2 M^{-1}. UV−vis [λ, nm (ε, M^{-1} cm^{-1})]: 495 (600), 310 (9400), 237 (18200).

*Synthesis of [Ru(I)$_2$(**HL2**)(CO)(PPh$_3$)] (**2A**).* To a pale-pink solution of [Ru(Cl)(H)(CO)(PPh$_3$)$_3$] (150 mg, 0.158 mmol) in degassed toluene (20 mL) was added under a N_2 atmosphere in an oven-dried Schlenk tube **HL2** (29 mg, 0.158 mmol), followed by ^{t}BuOK (53 mg, 0.473 mmol) and CH_2I_2 (64 μL, 0.79 mmol, 5 equiv). The solution was refluxed under an inert atmosphere overnight. The solution gradually turned yellow with progression of the reaction. Evaporation of the solvent under vacuum afforded a yellow solid, which was subjected to chromatographic purification using a neutral alumina column and 1:1 dichloromethane/petroleum ether as the eluent. Removal of the solvent under vacuum resulted in complexes **2** (85 mg, 55%) and **2A** (40 mg, 30%). Slow evaporation of its 2:1 dichloromethane/hexane solution gave yellow crystals of **2A**. MS (ESI$^+$, CH_3CN; {**2A** + H}$^+$). Calcd: m/z 829.89. Found: m/z 829.94. ^{1}H NMR (500 MHz, $CDCl_3$): δ 9.28 (d, J = 4.9 Hz, 1H), 7.98−7.79 (m, 6H), 7.51 (t, J = 7.6 Hz, 1H), 7.34 (dd, J = 20.9 and 6.4 Hz, 13H), 7.21 (d, J = 3.3 Hz, 2H), 6.57 (d, J = 7.9 Hz, 1H), 5.58 (t, 1H), 3.63 (t, J = 10.5 Hz, 1H), 2.48 (dd, 1H). ^{13}C NMR (126 MHz,

DOI: 10.1021/acs.inorgchem.9b03065
Inorg. Chem. XXXX, XXX, XXX−XXX

$CDCl_3$): δ 206.38, 163.71, 153.57, 140.31, 137.10, 135.27, 134.88, 133.86, 133.79, 129.90, 129.89, 129.68, 129.14, 128.31, 128.23, 128.15, 124.37, 124.35, 124.11, 124.09, 64.90. DEPT-135 (^{13}C NMR; 126 MHz, $CDCl_3$): δ 153.57, 137.10, 133.86, 133.79, 129.91, 129.89, 129.69, 129.14, 128.31, 128.23, 128.15, 124.37, 124.35, 124.11, 124.09, 64.90, 64.88. ^{31}P NMR (202 MHz, $CDCl_3$): δ 54.17. Anal. Calcd for $C_{31}H_{27}N_2O_1P_1I_2Ru$: C, 44.89; H, 3.28; N, 3.38. Found: C, 44.76; H, 3.25; N, 3.14. IR (KBr, cm^{-1}): 1942 [ν(C≡O)]. Molar conductivity (CH_3CN): Λ_M = 6 Ω^{-1} cm^2 M^{-1}. UV−vis [λ, nm (ε, M^{-1} cm^{-1})]: 351 (3600), 307 (17600), 241 (21200).

*Generation of Dianion (**DA**).* To a pale-pink solution of [Ru(Cl)(H)(CO)(PPh_3)$_3$] (150 mg, 0.158 mmol) in degassed toluene (20 mL) in an oven-dried Schlenk tube was added under a N_2 atmosphere **HL2** (29 mg, 0.158 mmol), followed by ^{t}BuOK (53 mg, 0.473 mmol). The solution was refluxed under an inert atmosphere for 4 h. The solution gradually turned green with progression of the reaction. Evaporation of the solvent under an inert atmosphere led to a green solid. This was further subjected to UV−vis (in degassed THF) and ^{1}H NMR (benzene-d_6) studies.

■ ASSOCIATED CONTENT

Ⓢ Supporting Information

The Supporting Information is available free of charge at https://pubs.acs.org/doi/10.1021/acs.inorgchem.9b03065.

MS spectra, crystal structures, NMR, GC−MS, crystallographic bond parameters, DFT-optimized structures, Gibbs free energy plot, and Cartesian coordinates (PDF)

Accession Codes

CCDC 1951286−1951293 contain the supplementary crystallographic data for this paper. These data can be obtained free of charge via www.ccdc.cam.ac.uk/data_request/cif, or by emailing data_request@ccdc.cam.ac.uk, or by contacting The Cambridge Crystallographic Data Centre, 12 Union Road, Cambridge CB2 1EZ, UK; fax: +44 1223 336033.

■ AUTHOR INFORMATION

Corresponding Authors

*Email: sanjibp@iitb.ac.in (S.P.).
*Email: lahiri@chem.iitb.ac.in (G.K.L.).

ORCID

Goutam Kumar Lahiri: 0000-0002-0199-6132

Notes

The authors declare no competing financial interest.

■ ACKNOWLEDGMENTS

Financial support received from the Science and Engineering Research Board (SERB, DST), J. C. Bose Fellowship (to G.K.L., SERB), CSIR (fellowship to S.P.), and UGC (fellowship to A.S.H.), New Delhi, India, is gratefully acknowledged. We are thankful to Prof. G. Rajaraman, Raju Saravanan, and Dipanjan Mandal (Department of Chemistry, IIT Bombay) for their help. We also gratefully acknowledge the valuable suggestions extended by the reviewers. Dedicated to Professor Sourav Pal, IISER-Kolkata on the occasion of his 65th birthday.

■ REFERENCES

(1) (a) Karlin, K. D. Model Offers Intermediate Insight. *Nature* **2010**, *463*, 168−169. (b) Gibson, S.; McGuire, R.; Rees, D. C. Principal Components Describing Biological Activities and Molecular Diversity of Heterocyclic Aromatic Ring Fragments. *J. Med. Chem.* **1996**, *39*, 4065−4072.

(2) (a) Zhang, B.; Studer, A. Recent Advances in the Synthesis of Nitrogen Heterocycles *via* Radical Cascade Reactions Using Isonitriles as Radical Acceptors. *Chem. Soc. Rev.* **2015**, *44*, 3505−3521. (b) Ray, R.; Chandra, S.; Yadav, V.; Mondal, P.; Maiti, D.; Lahiri, G. K. Ligand Controlled Switchable Selectivity in Ruthenium Catalyzed Aerobic Oxidation of Primary Amines. *Chem. Commun.* **2017**, *53*, 4006−4009. (c) Kim, S.; Ginsbach, J. W.; Lee, J. Y.; Peterson, R. L.; Liu, J. J.; Siegler, M. A.; Sarjeant, A. A.; Solomon, E. I.; Karlin, K. D. Amine Oxidative *N*-Dealkylation *via* Cupric Hydroperoxide Cu-OOH Homolytic Cleavage Followed by Site-Specific Fenton Chemistry. *J. Am. Chem. Soc.* **2015**, *137*, 2867−2874.

(3) (a) Engin, M. S.; Demir, S.; Direkel, S.; Eymur, S.; Cay, S.; Güder, A. Synthesis, Characterization, Biological Activity, and DFT-Reactivity Assessment of Mn(II), Co(II), and Cu(II) Complexes of a New N_2O Tridentate Schiff Base. *Russ. J. Gen. Chem.* **2016**, *86*, 2855−2861. (b) Xue, L.; Wang, H.-H.; Wang, X.-J.; Jiang, H. Modulating Affinities of Di-2-picolylamine (DPA)-Substituted Quinoline Sensors for Zinc Ions by Varying Pendant Ligands. *Inorg. Chem.* **2008**, *47*, 4310−4318.

(4) (a) Mirica, L. M.; Ottenwaelder, X.; Stack, T. D. P. Structure and Spectroscopy of Copper-Dioxygen Complexes. *Chem. Rev.* **2004**, *104*, 1013−104. (b) Peterson, R. L.; Himes, R. A.; Kotani, H.; Suenobu, T.; Tian, L.; Siegler, M. A.; Solomon, E. I.; Fukuzumi, S.; Karlin, K. D. Cupric Superoxo-Mediated Intermolecular C-H Activation Chemistry. *J. Am. Chem. Soc.* **2011**, *133*, 1702−1705. (c) Lewis, E. A.; Tolman, W. B. Reactivity of Dioxygen-Copper Systems. *Chem. Rev.* **2004**, *104*, 1047−1076.

(5) (a) Tejel, C.; del Río, M. P.; Ciriano, M. A.; Reijerse, E. J.; Hartl, F.; Zalis, S.; Hetterscheid, D. G. H.; Tsichlis i Spithas, N.; de Bruin, B. Ligand-Centred Reactivity of Bis(picolyl)amine Iridium: Sequential Deprotonation, Oxidation and Oxygenation of a "Non-Innocent" Ligand. *Chem. - Eur. J.* **2009**, *15*, 11878−11889. (b) Padhi, S. K.; Manivannan, V. $Cu(NO_3)_2{\cdot}3H_2O$-Mediated Synthesis of 4′-(2-Pyridyl)-2,2′:6′,2″-terpyridine (L2) from *N*-(2-Pyridylmethyl)-pyridine-2-methylketimine (L1). A C-C Bond-Forming Reaction and the Structure of $\{[Cu(L_2)(OH)(NO_3)][Cu(L_2)(NO_3)_2]\}{\cdot}2H_2O$. *Inorg. Chem.* **2006**, *45*, 7994−7996. (c) Gomez, J.; Garcıa-Herbosa, G.; Cuevas, J. V.; Arnaiz, A.; Carbayo, A.; Munoz, A.; Falvello, L.; Fanwick, P. E. Diastereospecific and Diastereoselective Syntheses of Ruthenium(II) Complexes Using N,N′ Bidentate Ligands Aryl-pyridin-2-ylmethyl-amine ArNH-CH_2-2-C_5H_4N and Their Oxidation to Imine Ligands. *Inorg. Chem.* **2006**, *45*, 2483−2493. (d) Rowland, J. M.; Olmstead, M. M.; Mascharak, P. K. Unusual Reactivity of Methylene Group Adjacent to Pyridine-2-Carboxamido Moiety in Iron(III) and Cobalt(III) Complexes. *Inorg. Chem.* **2002**, *41*, 2754−2760. (e) Klappa, J. J.; Rich, A. E.; McNeill, K. One-Step Synthesis of 3,5-Disubstituted-2-pyridylpyrroles from the Condensation of 1,3-Diones and 2-(Aminomethyl)pyridine. *Org. Lett.* **2002**, *4*, 435−437. (f) Anjana, S.; Donring, S.; Sanjib, P.; Varghese, B.; Murthy, N. N. Controlling the Oxidation of Bis-tridentate Cobalt(II) Complexes having Bis(2-pyridylalkyl)amines: Ligand vs. Metal Oxidation. *Dalton Trans.* **2017**, *46*, 10830−10836.

(6) Campbell, A. N.; Stahl, S. S. Overcoming the "Oxidant Problem": Strategies to Use O2 as the Oxidant in Organometallic C−H Oxidation Reactions Catalyzed by Pd (and Cu). *Acc. Chem. Res.* **2012**, *45*, 851−863.

(7) (a) Mandal, A.; Schwederski, B.; Fiedler, J.; Kaim, W.; Lahiri, G. K. Evidence for Bidirectional Noninnocent Behavior of a Formazanate Ligand in Ruthenium Complexes. *Inorg. Chem.* **2015**, *54*, 8126−8135. (b) Panda, S.; Bera, S.; Lahiri, G. K. Electronic Impact of Ancillary Ligand on the Oxygenation Profile of Ruthenium Coordinated β-Diketiminate. *Polyhedron* **2019**, *172*, 45−57. (c) Panda, S.; Ansari, M. A.; Mandal, A.; Lahiri, G. K. Near-IR Absorbing Ruthenium Complexes of Non-Innocent 6,12-Di(pyridin-2-yl)indolo[3,2-*b*]-carbazole: Variation as a Function of Co-Ligands. *Chem. - Asian J.* **2019**, *14*, 4631.

(8) (a) Rusanova, J.; Rusanov, E.; Gorelsky, S. I.; Christendat, D.; Popescu, R.; Farah, A. A.; Beaulac, R.; Reber, C.; Lever, A. B. P. The Very Covalent Diammino(*o*-benzoquinonediimine) Dichlororuthenium(II). An Example of Very Strong π-Back Donation. *Inorg. Chem.* **2006**, *45*, 6246−6262. (b) Rigo, M.; Hettmanczyk, L.;

DOI: 10.1021/acs.inorgchem.9b03065
Inorg. Chem. XXXX, XXX, XXX−XXX

Heutz, F. J. L.; Hohloch, S.; Lutz, M.; Sarkar, B.; Müller, C. Phosphinines versus Mesoionic Carbenes: A Comparison of Structurally Related Ligands in Au(I)-Catalysis. *Dalton Trans.* **2017**, *46*, 86−95.
(9) Nag, S.; Butcher, R. J.; Bhattacharya, S. *N*-(Aryl)picolinamide Complexes of Ruthenium: Usual Coordination and Strategic Cyclometalation. *Eur. J. Inorg. Chem.* **2007**, *2007*, 1251−1260.
(10) (a) Małecki, J. G.; Maron, A. A Ruthenium(II) Hydride Carbonyl Complex with 4-Phenylpyrimidine as Co-ligand. *Transition Met. Chem.* **2012**, *37*, 727−734. (b) Ghosh, P.; Panda, S.; Banerjee, S.; Lahiri, G. K. Ruthenium-Hydride Mediated Unsymmetrical Cleavage of Benzofuroxan to 2-Nitroanilido with Varying Coordination Mode. *Inorg. Chem.* **2017**, *56*, 10735−10747. (c) Kundu, S.; Dutta, D.; Maity, S.; Weyhermüller, T.; Ghosh, P. Proton-Coupled Oxidation of a Diarylamine: Amido and Aminyl Radical Complexes of Ruthenium-(II). *Inorg. Chem.* **2018**, *57*, 11948−11960.
(11) (a) Tejel, C.; Ciriano, M. A.; del Rio, M. P.; Hetterscheid, D. G. H.; Tsichlis i Spithas, N.; Smits, J. M. M.; de Bruin, B. Ligand Oxidation of a Deprotonated Bis(picolyl)amine Ir^{I}(cod) Complex. *Chem. - Eur. J.* **2008**, *14*, 10932−10936. (b) Olbert, D.; Görls, H.; Conrad, D.; Westerhausen, M. Coordination Behavior of the (Diphenylphosphanyl)[α-(2-pyridyl)benzyl]amide Anion toward Lithium and Zinc Cations. *Eur. J. Inorg. Chem.* **2010**, *2010*, 1791−1797.
(12) Kotani, H.; Sugiyama, T.; Ishizuka, T.; Shiota, Y.; Yoshizawa, K.; Kojima, T. Redox-Noninnocent Behavior of Tris(2-pyridylmethyl)amine Bound to a Lewis Acidic Rh(III) Ion Induced by C-H Deprotonation. *J. Am. Chem. Soc.* **2015**, *137*, 11222−11225.
(13) For the sake of simplicity in calculation, the energy of K^+ has been deducted at the product formation step instead of considering its involvement in each step. Further, because of the comparable dielectric constants of *tert*-butyl alcohol and 2-butanol, a computational study has been performed in a 2-butanol medium.
(14) (a) Tejel, C.; Ciriano, M. A.; del Rio, M. P.; van den Bruele, F. J.; Hetterscheid, D. G. H.; Tsichlis i Spithas, N.; de Bruin, B. Deprotonation Induced Ligand-to-Metal Electron Transfer: Synthesis of a Mixed-Valence Rh(-I,I) Dinuclear Compound and Its Reaction with Dioxygen. *J. Am. Chem. Soc.* **2008**, *130*, 5844−5845. (b) Panda, S.; Bera, S. K.; Goel, P.; Dutta, A. K.; Lahiri, G. K. Ruthenium-Chelated Non-Innocent Bis(heterocyclo)methanides: A Mimicked β-Diketiminate. *Inorg. Chem.* **2019**, *58*, 11458−11469.
(15) (a) Mikheikin, I. D.; Vorontsova, I. K.; Abronin, I. A. Reactivity of Molecular Oxygen on the Surface of Ionic Crystals. *Int. J. Quantum Chem.* **2002**, *88*, 489−495. (b) Moro-Oka, Y. Reactivities of Active Oxygen Species and Their Roles in the Catalytic Oxidation of Inactive Hydrocarbon. *Catal. Today* **1998**, *45*, 3−12.
(16) (a) Tang, J.; Gao, X. J.; Tang, H.; Zeng, X. Dioxygen Activation with Stable *N*-Heterocyclic Carbenes. *Chem. Commun.* **2019**, *55*, 1584−1587. (b) Reddy, A. R.; Bendikov, M. Diels-Alder Reaction of Acenes with Singlet and Triplet Oxygen-Theoretical Study of Two-State Reactivity. *Chem. Commun.* **2006**, 1179−1181. (c) Panda, S.; Mandal, A.; Ghosh, P.; Lahiri, G. K. Ru-Complex Framework toward Aerobic Oxidative Transformations of β-Diketiminate and α-Ketodiimine. *Inorg. Chem.* **2017**, *56*, 14900−14911.
(17) Ginsbach, J. W.; Peterson, R. L.; Cowley, R. E.; Karlin, K. D.; Solomon, E. I. Correlation of the Electronic and Geometric Structures in Mononuclear Copper(II) Superoxide Complexes. *Inorg. Chem.* **2013**, *52*, 12872−12874.
(18) (a) Baldwin, J. E. Rules for ring closure. *J. Chem. Soc., Chem. Commun.* **1976**, 734−736. (b) Alabugin, I. V.; Gilmore, K.; Manoharan, M. Rules for Anionic and Radical Ring Closure of Alkynes. *J. Am. Chem. Soc.* **2011**, *133*, 12608−12623.
(19) (a) Ishigaki, Y.; Shimajiri, T.; Takeda, T.; Katoono, R.; Suzuki, T. Longest C-C Single Bondamong Neutral Hydrocarbonswith a Bond Length beyond 1.8 Å. *CHEM* **2018**, *4*, 795−806. (b) Schreiner, P. R.; Chernish, L. V.; Gunchenko, P. A.; Tikhonchuk, E. Yu.; Hausmann, H.; Serafin, M.; Schlecht, S.; Dahl, J. E. P.; Carlson, R. M. K.; Fokin, A. A. Overcoming Lability of Extremely Long Alkane Carbon-Carbon Bonds Through Dispersion Forces. *Nature* **2011**, *477*, 308−311. (c) Gunbas, G.; Hafezi, N.; Sheppard, W. L.; Olmstead, M. M.; Stoyanova, I. V.; Tham, F. S.; Meyer, M. P.; Mascal, M. Extreme oxatriquinanes and a record C−O bond length. *Nat. Chem.* **2012**, *4*, 1018−1023.
(20) Bera, S. K.; Panda, S.; Dey Baksi, S.; Lahiri, G. K. Diverse Modes of Functionalisation of Ruthenium Coordinated β-Ketoiminate Analogues. *Dalton Trans.* **2018**, *47*, 15897−15906.
(21) Ahmad, N.; Levison, J. J.; Robinson, S. D.; Uttley, M. F.; Wonchoba, E. R.; Parshall, G. W. Complexes of Ruthenium, Osmium, Rhodium, and Iridium Containing Hydride Carbonyl, or Nitrosyl Ligands. *Inorg. Synth.* **2007**, *15*, 45−64.
(22) Goswami, S.; Chakravarty, A. R.; Chakravorty, A. Chemistry of Ruthenium. 2. Synthesis, Structure, and Redox Properties of 2-(Arylazo)pyridine Complexes. *Inorg. Chem.* **1981**, *20*, 2246−2250.
(23) Wang, Y.; Liu, H.; Zhang, X.; Zhang, Z.; Huang, D. Experimental and Mechanistic Insights into Copper(II)−dioxygen Catalyzed Oxidative *N*-Dealkylation of *N*-(2-Pyridylmethyl) phenylamine and Its Derivatives. *Org. Biomol. Chem.* **2017**, *15*, 9164−9168.
(24) Olbert, D.; Görls, H.; Conrad, D.; Westerhausen, M. Coordination Behavior of the Diphenylphosphanyl)[α-(2-pyridyl)-benzyl]amide Anion toward Lithium and Zinc Cations. *Eur. J. Inorg. Chem.* **2010**, *2010*, 1791−1797.
(25) Qi, G.; Ji, Y. Q.; Judeh, Z. M. A. Novel Chiral C_1-1′,2′,3′,4′-Tetrahydro-1,10-bisisoquinolines: Synthesis, Resolution, and Applications in Catalytic Enantioselective Reactions. *Tetrahedron* **2010**, *66*, 4195−4205.
(26) Lake, B. R. M.; Shaver, M. P. Iron(II) β-Ketiminate Complexes as Mediators of Controlled Radical Polymerization. *Dalton Trans.* **2016**, *45*, 15840−15849.
(27) (a) Sheldrick, G. M. *Acta Crystallogr., Sect. A: Found. Crystallogr.* **2008**, *A64*, 112−122. (b) Sheldrick, G. M. *Program for Crystal Structure Solution and Refinement*; University of Goettingen: Goettingen, Germany, 1997. (c) Sheldrick, G. M. Crystal structure refinement with SHELXL. *Acta Crystallogr., Sect. C: Struct. Chem.* **2015**, *71*, 3−8.
(28) Lee, C.; Yang, W.; Parr, R. G. Development of the Colle-Salvetti Correlation-Energy Formula into a Functional of the Electron Density. *Phys. Rev. B: Condens. Matter Mater. Phys.* **1988**, *37*, 785−789.
(29) (a) Andrae, D.; Haeussermann, U.; Dolg, M.; Stoll, H.; Preuss, H. Energy-adjusted *ab initio* Pseudo Potentials for the Second and Third row Transition Elements. *Theor. Chim. Acta* **1990**, *77*, 123. (b) Fuentealba, P.; Preuss, H.; Stoll, H.; von Szentpaly, L. Proper Account of Core-Polarization with Pseudopotentials: Single Valence-Electron Alkali Compounds. *Chem. Phys. Lett.* **1982**, *89*, 418.
(30) Frisch, M. J.; Trucks, G. W.; Schlegel, H. B.; Scuseria, G. E.; Robb, M. A.; Cheeseman, J. R.; Scalmani, G.; Barone, V.; Mennucci, B.; Petersson, G. A.; Nakatsuji, H.; Caricato, M.; Li, X.; Hratchian, H. P.; Izmaylov, A. F.; Bloino, J.; Zheng, G.; Sonnenberg, J. L.; Hada, M.; Ehara, M.; Toyota, K.; Fukuda, R.; Hasegawa, J.; Ishida, M.; Nakajima, T.; Honda, Y.; Kitao, O.; Nakai, T.; Vreven, T.; Montgomery, J. A., Jr; Peralta, J. E.; Ogliaro, F.; Bearpark, M.; Heyd, J. J.; Brothers, E.; Kudin, K. N.; Staroverov, V. N.; Kobayashi, R.; Normand, J.; Raghavachari, K.; Rendell, A.; Burant, J. C.; Iyengar, S. S.; Tomasi, J.; Cossi, M.; Rega, N.; Millam, J. M.; Klene, M.; Knox, J. E.; Cross, J. B.; Bakken, V.; Adamo, C.; Jaramillo, J.; Gomperts, R.; Stratmann, R. E.; Yazyev, O.; Austrin, A. J.; Cammi, R.; Pomelli, C.; Ochterski, J. W.; Martin, R. L.; Morokuma, K.; Zakrzewski, V. G.; Voth, G. A.; Salvador, P.; Dannenberg, J. J.; Dapprich, S.; Daniels, A. D.; Farkas, Ö.; Foresman, J. B.; Ortiz, J. V.; Cioslowski, J.; Fox, D. J. *Gaussian 09*, revision A.02; Gaussian, Inc.: Wallingford, CT, 2009.
(31) Zhurko, D. A.; Zhurko, G. A. *ChemCraft 1.5*; Plimus: San Diego, CA. Available at http://www.chemcraftprog.com.

DOI: 10.1021/acs.inorgchem.9b03065
Inorg. Chem. XXXX, XXX, XXX−XXX